Electronic Supplementary Material (ESI) for Chemical Science.

Supplementary Information

1. Organic synthesis

General information: reagents, solvents and reference standards of some possible photoproducts were purchased from TCI and Sigma Aldrich (Merck), carbon ^{13}C-enriched potassium thiocyanate-^{13}C from Sigma Aldrich (Merck) and phenol-$^{13}C_6$ from Toronto Research Chemicals. For TLC ALUGRAM® Xtra SIL aluminum sheets from Macherey-Nagel were used. Column chromatography was done on Macherey-Nagel silica gel 60 (particle size 0.04-0.06 mm). NMR spectra were measured on a Bruker AV 500 MHz device. Spectra were referenced to the DMSO-d_6 peak using the following values: ^1H 2.50, ^{13}C 39.52. The solvent was purchased at Eurisotop. Chemical shifts (δ) are reported on a ppm scale. Following abbreviations were used to describe multiplicities: s = singlet, d = doublet, m = multiplet. Coupling constants (*J*) are reported in Hertz (Hz). High-Resolution Mass Spectrometry was performed on MALDI-LTQ Orbitrap XL™ device from Thermo Fisher Scientific.

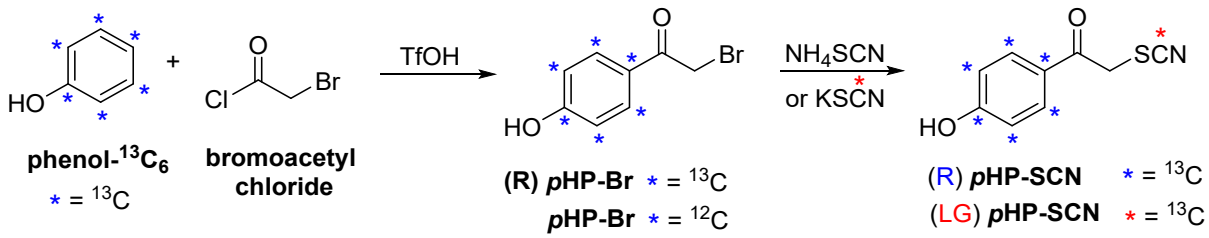

Figure S1: Synthesis overview of the ring (Ring) and leaving group (LG) ^{13}C labelled *p*HP-SCN.

2. Synthesis descriptions

a. (R) *p*HP-Br

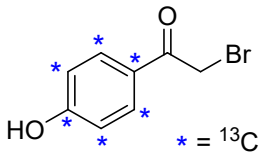

Figure S2. Chemical structure of 2-Bromo-4'-hydroxyacetophenone-$^{13}C_6$.

Phenol-$^{13}C_6$ (235 mg, 2.35 mmol, 1.00 eq) was dissolved in trifluoromethanesulfonic acid (TfOH)[44] and cooled in ice bath before the addition of bromoacetyl chloride (388 mg, 2.46 mmol, 1.05 eq). After 15 min the cooling bath was removed and the mixture was stirred in room temperature overnight. The reaction was quenched by pouring it in ice water, then filtrated. The white solid on the filter and the aqueous layer was washed with cyclohexane (which predominantly dissolves the side product 2-bromo-2'-hydroxyacetophenone-$^{13}C_6$). Then, the white residue on the filter was dissolved in EtOAc and the aqueous layer was extracted 2 x with EtOAc. Both EtOAc fractions were combined, washed with saturated $NaHCO_3$, 2 x with brine, dried over Na_2SO_4 and filtered. The solvent was removed under reduced pressure to give 344 mg of crude material, which was practically pure product (66%). However, to obtain an analytically pure sample, column chromatography was used (SiO_2, eluent Cy : EtoAc 3:1). The NMR sample was prepared directly before measurement to avoid spectra contaminations by signals resulting from the compound degradation in the NMR solvent. ^1H (500 MHz, DMSO-d_6): δ 10.55-10.51 (m, 1H), 8.08-8.00 (m, 1H), 7.76-7.68 (m, 1H), 7.06-6.99 (m, 1H), 6.73-6.67 (m, 1H), 4.78 (s, 2H) ppm. ^{13}C (125 MHz, DMSO-d_6): δ 190.3-189.6 (m), 163.2-162.0 (m, ^{13}C), 132.0-130.9 (m, ^{13}C), 125.9-124.8 (m, ^{13}C), 116.0-114.8 (m, ^{13}C), 33.6 (d, $^3J_{CC}$ = 17.7 Hz) ppm.

b.(Ring) *p*HP-SCN

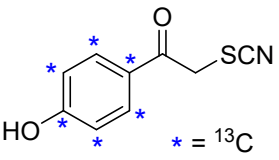

Figure S3. Chemical structure of 2-Thiocyano-4'-hydroxyacetophenone-$^{13}C_6$.

2-bromo-4´-hydroxyacetophenone-$^{13}C_6$ prepared in the previous step (190 mg, 0.86 mmol) and NH_4SCN (131 mg, 1.72 mmol) were dissolved in a mixture of EtOH and H_2O (2 mL, 2:1) and stirred at room temperature overnight (white precipitate formed). The reaction was diluted by water and EtOAc, organic phase separated, the aqueous layer was extracted with EtOAc. Combined organic phase was washed 2 x with brine, dried over Na_2SO_4 and filtered. Solvent was removed under reduced pressure. The crude product was crystalized from EtOAc/Cy to give 101 mg of product, the filtrate was purified by column chromatography (SiO_2, Cy:EtOAc 3:1) to give additional 58 mg of the product. The combined mass of the product **(Ring) *p*HP-SCN** was 159 mg (93%). ^{1}H (500 MHz, DMSO-d_6): δ 10.63-10.58 (m, 1H), 8.08-8.00 (m, 1H), 7.76-7.69 (m, 1H), 7.08-7.00 (m, 1H), 6.76-6.68 (m, 1H), 5.02 (s, 2H) ppm. ^{13}C (125 MHz, DMSO-d_6): δ 190.6-189.9 (m), 163.6-162.5 (m, ^{13}C), 131.9-130.8 (m, ^{13}C), 126.2-125.2 (m, ^{13}C), 116.0-114.9 (m, ^{13}C), 113.0, 41.7 (d, $^2J_{CC}$ = 16.6 Hz) ppm. HRMS (MALDI) m/z: $[M+H]^+$ Calc. for $C_3{}^{13}C_6H_8N_1O_2S_1$ 200.04715; Found 200.04718.

c. (LG) ***p*HP-SCN**

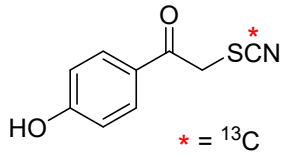

Figure S4. Chemical structure of 2-Thiocyano(-^{13}C)-4'-hydroxyacetophenone.

Synthesis was done as described for ring labelled compound using commercially available 2-bromo-4´-hydroxyacetophenone (***p*HP-Br**, 571 mg, 2.67 mmol, 1.05 eq) and K^{13}CN (250 mg, 2.54 mmol, 1.00 eq). The crude product (538 mg) was crystalized from EtOAc/Cy to give 317 mg (64%) of pure product. ^{1}H (500 MHz, DMSO-d_6): δ 10.61 (s, 1H), 7.91-7.86 (m, 2H), 6.90-6.86 (m, 2H), 5.02 (d, 1H, J_{1H13C} = 4.6 Hz) ppm. ^{13}C (125 MHz, DMSO-d_6): δ 190.3 (d, $^3J_{CC}$ = 2.6 Hz), 163.1, 131.4, 125.8, 115.5, 113.1 (^{13}C), 41.7 ppm. HRMS (MALDI) m/z: $[M+H]^+$ Calc. for $C_8{}^{13}C_1H_8N_1O_2S_1$ 195.03038; Found 195.03006.

d. ***p*HP-SCN**

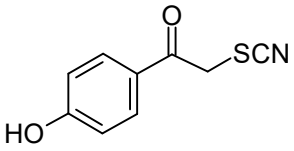

Figure S5. Chemical structure of 2-thiocyano-4'-hydroxyacetophenone

pHP-Br (428 mg, 2.00 mmol, 1.00 eq) and NH_4SCN (304 mg, 4.00 mmol, 2.00 eq) were dissolved in a mixture of EtOH and H_2O (2 mL, 2:1) and stirred at room temperature overnight. Then the mixture was poured on ice and filtrated. The crude product (344 mg) was recrystalised from EtOAc/Cy to give 191 mg of pure white solid (49%). ^{1}H (500 MHz, DMSO-d_6): δ 10.61 (s, 1H), 7.91-7.87 (m, 2H), 6.90-6.86 (m, 2H), 5.02 (s, 2H) ppm. ^{13}C (125 MHz, DMSO-d_6): δ 190.3, 163.1, 131.4, 125.8, 115.5, 113.1, 41.7 ppm. HRMS (MALDI) m/z: $[M+H]^+$ Calc. for $C_9H_8N_1O_2S_1$ 194.02703; Found 194.02690.

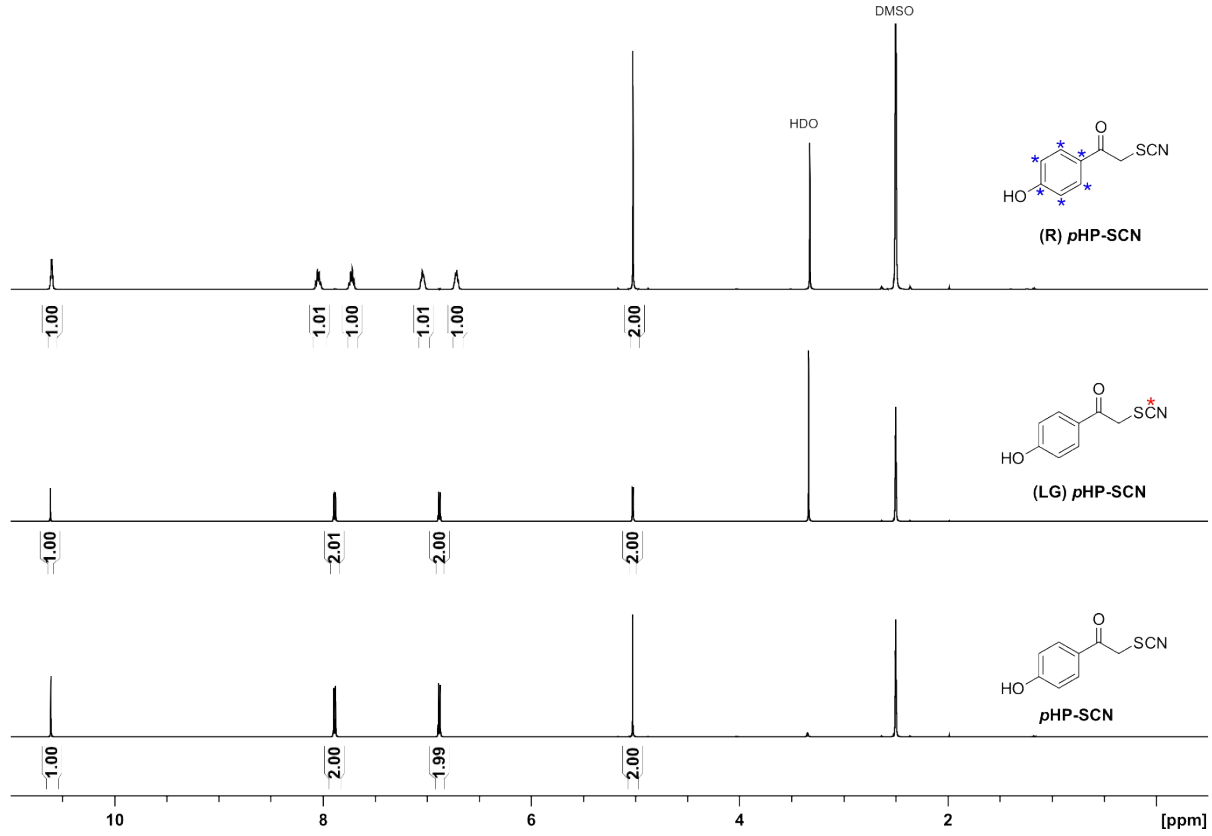

Figure S6: ^{1}H (500 MHz, DMSO-d_6) spectra of **(Ring) pHP-SCN** and **(LG) pHP-SCN**, and ***p*HP-SCN**.

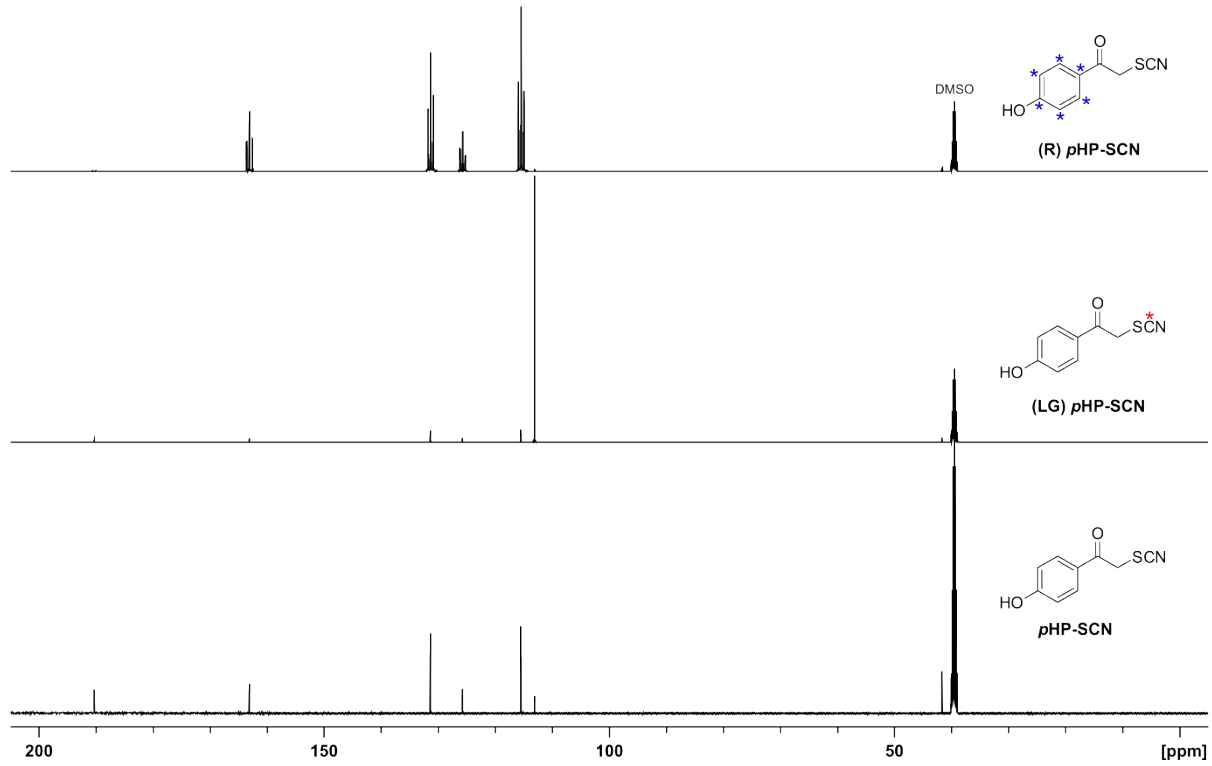

Figure S7. ^{13}C (125 MHz, DMSO-d_6) spectra of **(Ring) pHP-SCN** and **(LG) pHP-SCN**, and ***p*HP-SCN**.

3. Steady-state spectroscopy of *p*HP-SCN and related compounds

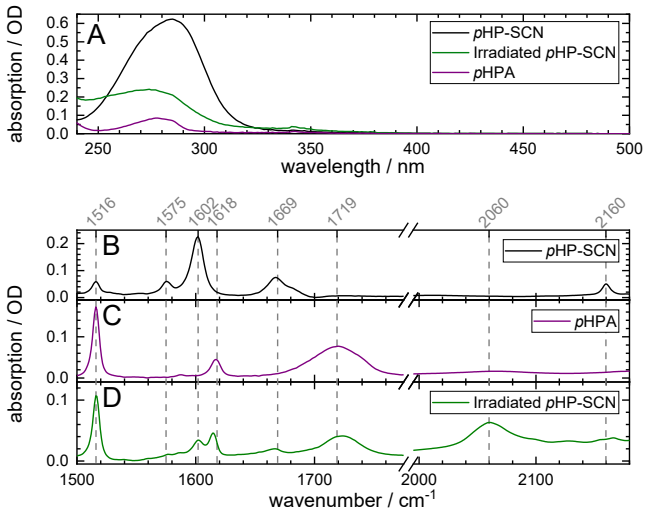

Figure S8. Steady-state UV/VIS and FTIR absorption spectra of *p*HP-SCN before and after radiation in 1:8 D_2O:MeCN. The spectra of the *p*HPA photoproduct are also shown. The data in panel A is measured in a quartz cuvette of 1 mm using a concentration of about 0.5 mM (at 253-nm excitation), panels B-D contained about 30 mM in a CaF_2 cell with a 50 µm teflon spacer. Panel D shows the spectrum of *p*HP-SCN spectrum after irradiation with 253 nm. The first ring mode at 1516 cm^{-1} gains intensity with respect to *p*HP-SCN, the next two ring modes become smaller. A positive band appears at 1618 cm^{-1}. The carbonyl band at 1669 cm^{-1} decreases markedly and a broad red-shifted product grows in at 1719 cm^{-1}. At 2060 cm^{-1} the released solvated SCN^- appears, while the bound SCN band around 2160 cm^{-1} has concomitantly decreased. Not all *p*HP-SCN is converted, as the bound SCN feature still has some intensity at the end of the illumination period. The product bands are all consistent with SCN^- being released and *p*HPA being the main reaction product (see also Figure S9 for FTIR spectra of structurally similar compounds). Other photoproducts and intermediates mainly occur in the absence of water, but for the purpose of this study we focus on the initial cleavage reaction in presence of water.[15,21]

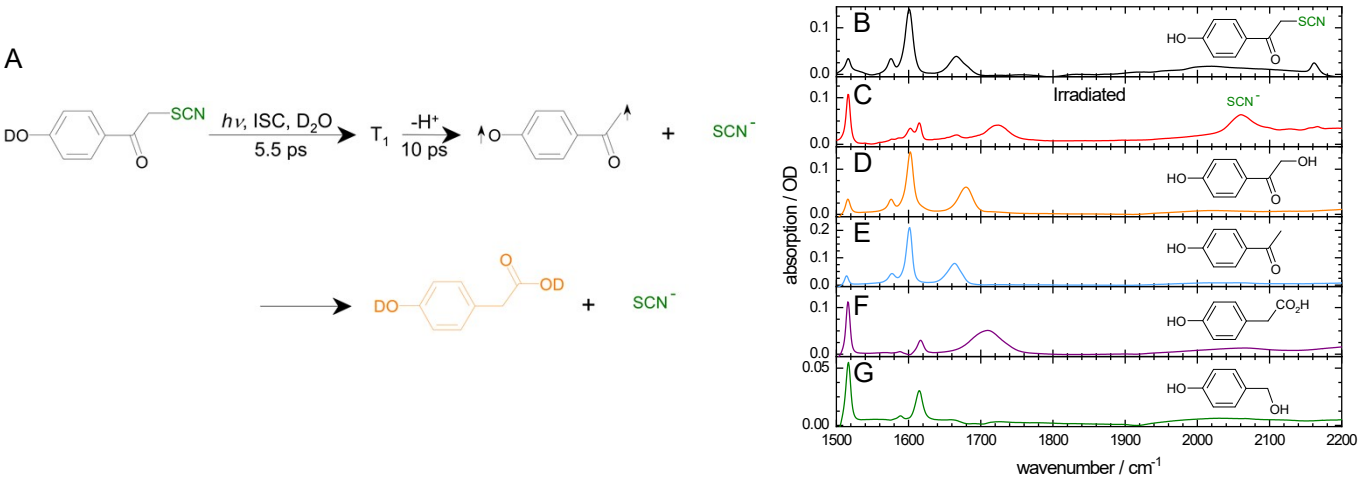

Figure S9. Proposed reaction mechanism after irradiation in presence of water. The scheme in panel A is adapted from refs. [15,21], the shown time constants are based on this work. Panels B-G show the steady-state FTIR spectra of the compound before (B) and after (C) irradiation, as well as those of the main *p*HPA photoproduct (D) and other structurally similar compounds for comparison (E-G). In panel C the feature of the released SCN anion is separately marked. The used solvent was 1:1 D_2O:MeCN. ISC stands for intersystem crossing, T_1 for the triplet.

4. Assignment of IR modes in *p*HP-SCN

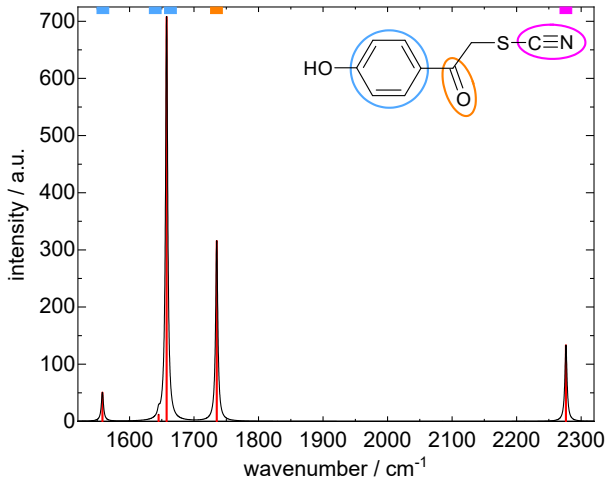

Figure S10. Computed vibrational frequencies of pHP-SCN before (red sticks) and after (black spectrum) convolution with 4 cm^{-1} wide Lorentzians. The spectral features are assigned to the dominant contributions of the vibrational modes, depicted by the colors in the corresponding chemical structure (ring modes in blue, carbonyl in orange, nitrile in pink).

5. Time-resolved spectroscopy of *p*HP-SCN in D_2O:MeCN 1:8

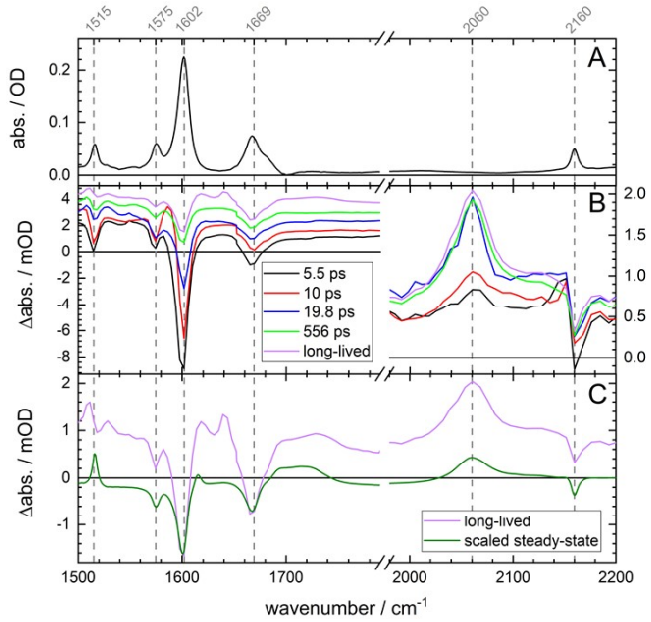

Figure S11. Reproduction of Figure 1, but with panel B including an offset of +0.8 mOD to each spectrum below 1800 cm^{-1} for improved readability. The signals in the SCN region contain no added offset, but are plotted on a different ordinate (shown to the right of the axis).

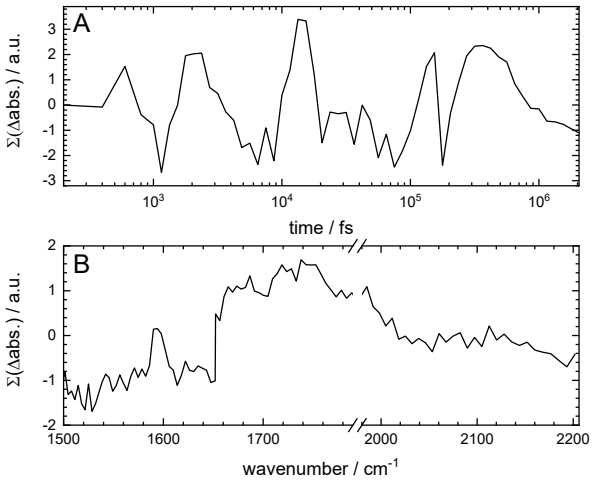

Figure S12. Residuals of the fit to the SADS of Figure 1. Panel A shows the sum of the residuals in time, panel B those over the wavenumber range. The structureless residuals are taken as measure for the quality of the fit.

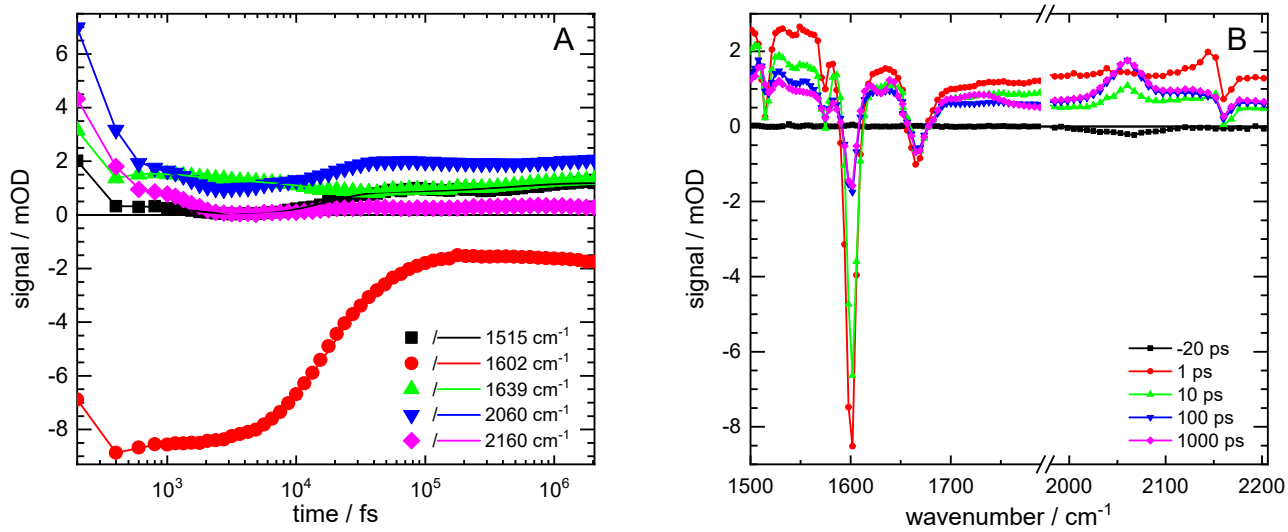

Figure S13. Raw data of Figure 1. Panel A shows time traces of the raw data (symbols) and their GA fits (continuous lines) of some main spectral features. Panel B shows a selection of measured spectral slices at several pump-probe delays. The symbols are the data points.

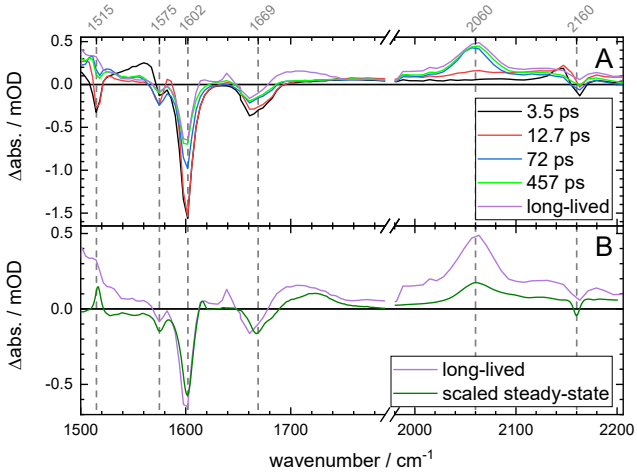

6. Time-resolved spectroscopy of *p*HP-SCN in D_2O:MeCN 1:1

Figure S14: SADS resulting from global analysis of 30 mM *p*HP-SCN (50 μm spacer) in 1:1 D_2O:MeCN after 2 μJ/pulse excitation at 266 nm. The legend shows the associated time constants. Two additional components are needed to fit the coherent artefact around time zero (not shown). Panel B compares the final SADS of A to a scaled FTIR light-induced difference spectrum. Figure S15 shows a selection of raw data in the form of time traces and their GA fits. In Figure S16 the residuals of the fit in time and over the wavenumber range are shown.

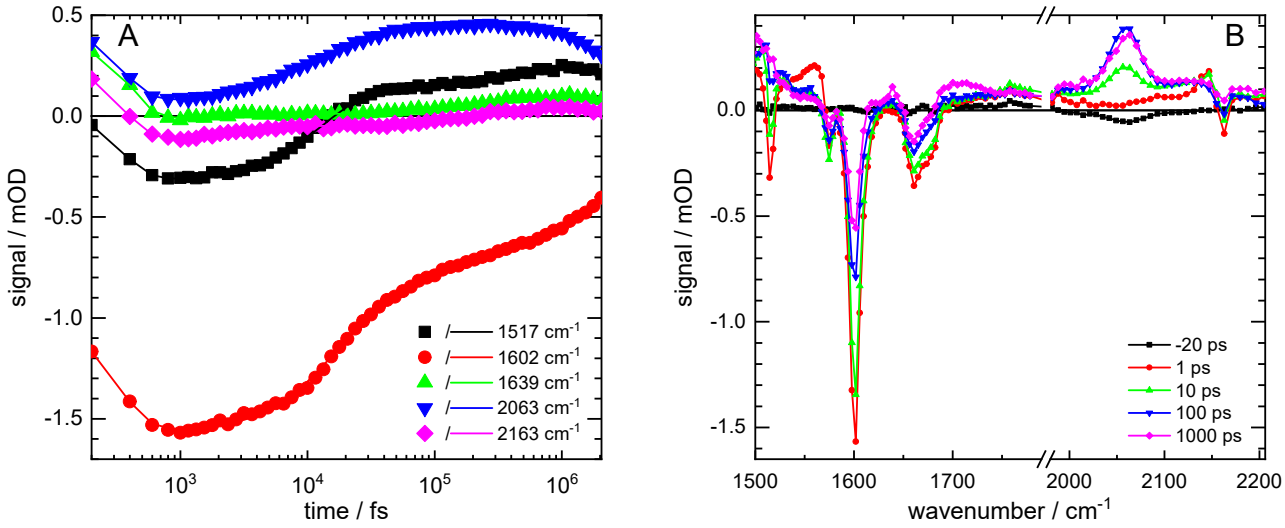

Figure S15. Raw data of Figure S14. Panel A shows time traces of the raw aw data (symbols) and their GA fits (continuous lines) of some main spectral features. Panel B shows a selection of measured spectral slices at several pump-probe delays. The symbols are the data points.

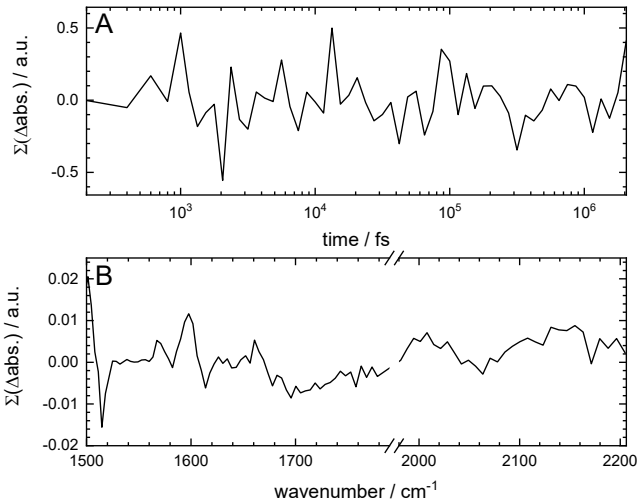

Figure S16. Residuals of the fit to the SADS of Figure S14. Panel A shows the sum of the residuals in time, panel B those over the wavenumber range. The structureless residuals are taken as measure for the quality of the fit.

7. Steady-state spectroscopy on the 50:50 isotopologue mixture

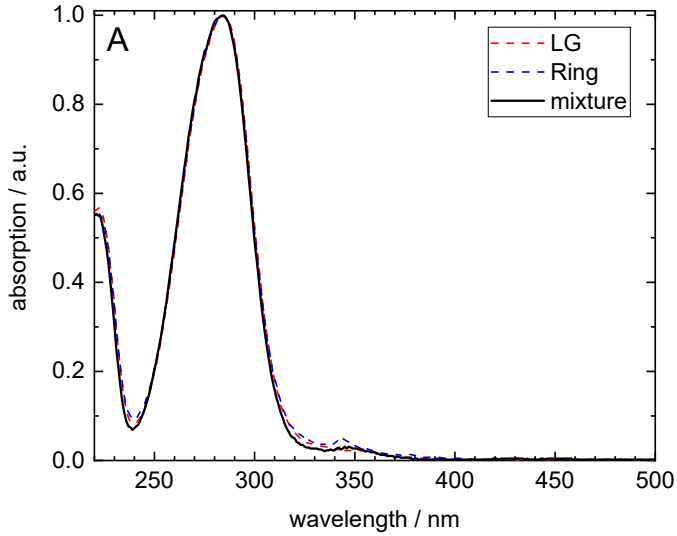

Figure S17. Comparison of UV/VIS spectra of the LG-labelled photocage, the ring-labelled photocage, and a 50:50 mixture of the two in 1:8 D_2O:MeCN. The normalized UV/VIS absorption spectra show a negligible influence on the peak wavelengths. The small feature around 345 nm is attributed to the presence of a small amount of deprotonated compound.[52] Spectral selection using visible excitation is impossible.

8. Computations of the VIPER effect for the isotopologues

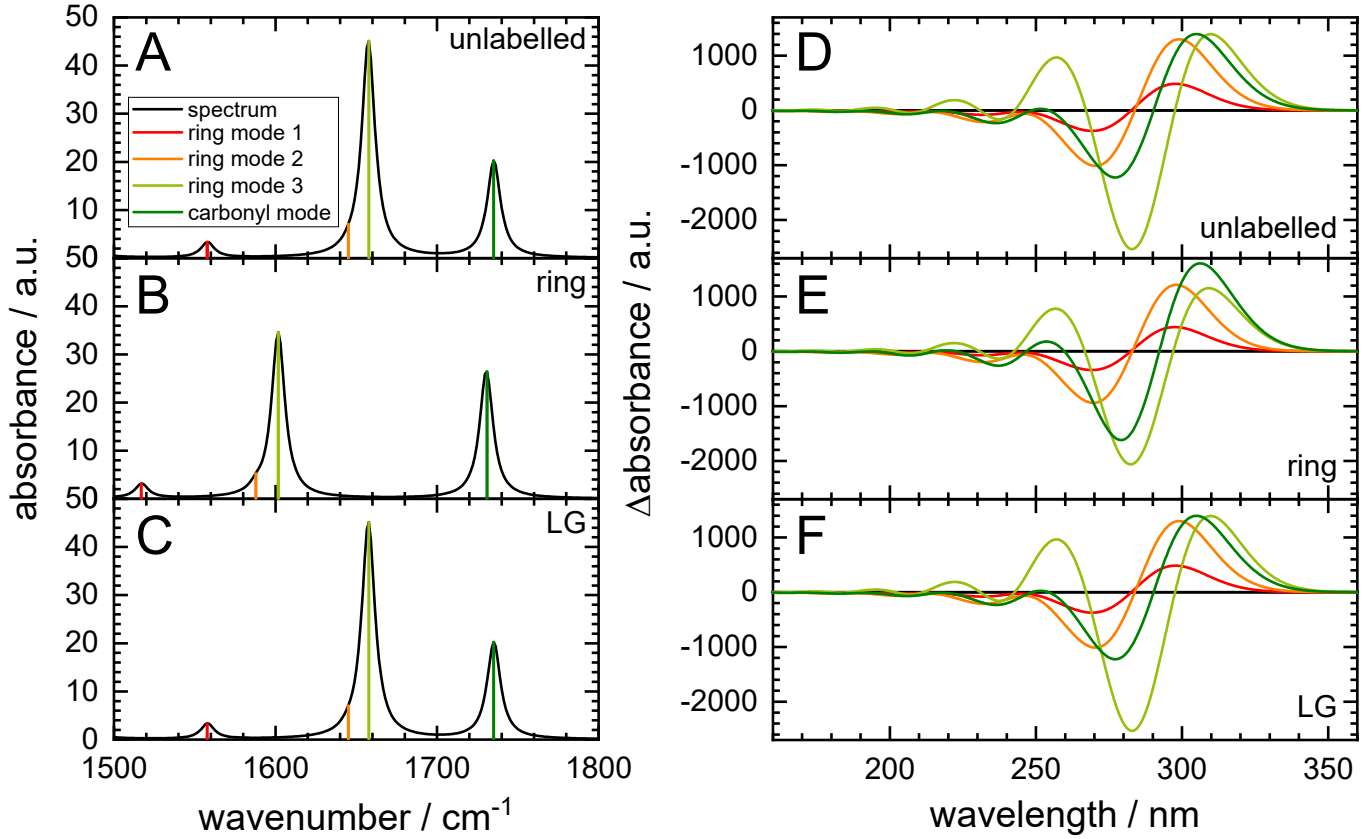

Figure S18. Theoretical prediction of the VIPER effect for different vibrational modes. Panels A-C show the computed IR spectra of the non-labelled, ring-labelled and LG-labelled isotopologues, respectively. Each mode is numbered and assigned (as shown in the legend of Panel A) and represented by a coloured stick. The black spectrum is the result of a convolution of the computed modes with a Lorentzian envelope function to match the experimental spectrum. Panels D-F show the shifts of the computed UV/VIS spectra for the same compounds, induced by vibrational pre-excitation of a particular vibrational mode. The color of each spectrum corresponds to the pre-excitation of the respective mode, where the colors are chosen as assigned in panel A. The absorption spectra themselves are convoluted by a Gaussian envelope function with a HWHM of 0.2 eV and wavenumber-shifted to match the width and location of the experimentally observed spectra. The shifts are then computed by subtracting the UV/VIS spectrum without a vibrational pre-excitation. These difference spectra are shown in panels D-F. The depicted results are obtained by employing the functional and basis set combination PBE0/Def2-TZVP and including solvent effects of MeCN *via* CPCM.